BNL-NUREG-37614
CONF-851203--2

# Investigation of Intergranular Stress Corrosion Cracking in the Fuel Pool at Three Mile Island Unit 1

BNL-NUREG--37614

TI86 006873

Carl J. Czajkowski
Brookhaven National Laboratory
Upton, New York 11973

ABSTRACT

An intergranular stress corrosion cracking failure of 304 stainless steel pipe in 2000 ppm B as $H_3BO_3$ + $H_2O$ at 100°C has been investigated. Constant extension rate testing has produced an intergranular type failure in material in air. Chemical analysis was performed on both the base metal and weld material, in addition to fractography, EPR testing and optical microscopy in discerning the mode of failure.
Various effects of $Cl^-$, $O_2$ and MnS are discussed. The results have indicated that the cause of failure was the severe sensitization coupled with probable contamination by S and possibly by Cl ions.

INSPECTIONS OF PIPING in the Three Mile Island Unit #1 spent fuel system in April 1979 revealed five through wall cracks near welded joints. Reports indicated that the cracks were circumferential in nature and located in the weld heat-affected zone adjacent to girth welds. Several months later, two more through wall cracks were detected in the spent fuel system which were reported as having the same cracking characteristics as the first five leaking welds.

In order to analyze the cracking phenomena in more detail, a section of radioactively contaminated 8" diameter pipe was sent to Brookhaven National Laboratory (BNL). The pipe (H.T. #334165) measured approximately 30" in length and contained two circumferential welds, SF 265 (through wall cracked-field weld), and SF 261 (uncracked-shop weld), as well as three uncracked longitudinal seam shop welds (Figure 1). (Note: Six of the seven through wall cracks were from material of this heat number 334165.)

The following program was initiated to analyze the failure:

1) Visual inspections and photographs of both the inner and outer surfaces
2) Optical microscopy
3) Scanning Electron Microscopy (SEM)
4) Energy Dispersive Spectroscopy (EDS)
5) Bulk chemistry of weld metal/base materials
6) Constant Extension Rate Testing (CERT)
7) Electrochemical Potentiokinetic Reactivation Analyses (EPR)

## EXAMINATIONS

VISUAL/PHOTOGRAPHY - Preliminary visual examination of the pipe disclosed that the crack (near SF 265) was adjacent to what appeared to be a weld repair area. In addition, GPU also communicated that the weld was a single "V" type with a shallow (= 20°) edge preparation. The filler metal used was an E308 Grinnell Consumable Insert and welded with ER308 electrode (Table 1). The welding process used was GTAW (Gas Tungsten Arc Welding). The repair area was in its R-2 stage (two repairs completed). The pipe had also been counterbored prior to installation for ease in pipe fit-up prior to welding. The crack on the outside surface of the pipe was approximately five inches long, ran parallel to the girth weld and was reasoned to be in the weld heat-affected zone. The pipe was then longitudinally sectioned and the inside surface visually inspected. The inside of the pipe contained a crack 5.5" long running parallel to the girth weld for half its length, with its direction varying into the counterbore at its terminal ends (Figure 2). The inside surface was covered with an oxide film and showed evidence of significant heating during welding. Eight sections were then cut bracketing the crack to facilitate further examinations.

OPTICAL MICROSCOPY - One specimen was cut and mounted in epoxy in such a manner that the cross section of the pipe's circumference was perpendicular to the plane of examination. The surface was polished and then electrolytically etched with a 10% oxalic acid etch for macrostructural depiction. The weld insert, weld deposit, crack and counterbore area are well defined showing the through wall crack and a smaller non-through wall crack on the weld side of the main crack (Figure 3). The specimen was then repolished and examined after ASTM A-262 Practice A was performed. As can be seen from the photomicrograph (Figure 4), the crack was intergranular in nature with secondary cracks branching out from the body of the main crack. The microstructure across the face of the specimen showed a fine grained structure in the pipe's central cross section, with increasing grain size outward towards the pipe's outside and inside surfaces. This grain size variance was visible in the specimen outside the weld HAZ, which may be the result of cold working operations prior to the solution annealing heat treatment in the pipe's manufacture. The area surrounding the crack and in the heat-affected zone exhibited a ditched structure (ASTM A262), which is evidence of considerable material sensitization. In view of the above observations, the failure is considered to be intergranular stress corrosion cracking in the sensitized region of the weld repair heat-affected zone.

Examination of the base material outside of the heat-affected zone after the ASTM A262 Practice A test revealed virtually no evidence of material sensitization, which would indicate that proper heat treatment (solution annealing) was applied by the supplier.

There were also a few indications of incipient cracking on the inside surface of the weldment in the counterbore area. These indications were visible on the counterbore of both the cracked side of the weld and the uncracked side.

Microscopy also discerned the appearance of stringer-like inclusions throughout the specimen's cross section. Later examination (EDS) disclosed these stringers to be MnS.

SEM/EDX - In an effort to identify any corrosive species present and to further evaluate the mode of cracking, various cracks were opened and the fracture faces evaluated by Scanning Electron Microscopy. The fracture faces examined had a coarsened grain structure at both the inner and outer edges of the specimens' cross sections with a finer grain structure at their mid-sections, similar to that found by optical microscopy. The fracture faces also had a typically intergranular stress corrosion cracking topography.

Several Energy Dispersive X-ray Spectroscopy (EDS) scans were made across the fracture face of the specimen in order to determine qualitatively the species present. The normal components of Type 304 stainless steel, Fe, Cr and Ni, were present with trace amounts of Al, Si, S and Ca present in many of the scans. In addition, chlorine (Cl) was present in trace amounts on the fracture surface near the inner surface of the piping.

Various particulates in the fracture face were also examined by EDS. Typically, in addition to Fe, Cr and Ni they also contained traces of Si and S, while some had traces of Cl, Ca and K present.

An examination was also made of the inner surface of the pipe where there appeared to be etched grain boundaries (Figure 5). The base metal adjacent to the grain boundary etching showed Al, Si, S, Ca and a trace of Cl in the scan (Figure 6).

EDS scans were then performed on the stringer-like inclusions which were originally discerned by optical microscopy. The scans showed both high S and Mn peaks (probably MnS) and at least one scan exhibited a Ti peak.

CHEMISTRY - Table 1 shows the results of chemical analyses on the base material and weld metal. Since the carbon content was higher than specifications allowed, two more specimens from the base metal were sent out to an independent laboratory for analysis. The additional two samples were both within specification for alloying elements of 304SS. The weld metal analysis varied somewhat from those reported by GPU, specifically in the carbon and chromium contents of the weldment. The disparities could have been caused by the difference in the testing methods used or possible constituent segregation in the material.

CONSTANT EXTENSION RATE TESTING - In order to investigate further the environmental conditions under which the weldment/pipe would fail, various tensile-type specimens were cut from the remaining material in both the field and shop welds. These specimens were subjected to constant extension rate tests (CERT) in various environments. The CERT method is basically the application of slow dynamic straining to a stress corrosion (tensile type) specimen while it is exposed to the environment. This particular mode of testing has the advantage of always resulting in a fracture at its completion and normally does so in a relatively short period of time (a few days). Another advantage of this type of testing is the ability to adjust the strain rate in the most probable range of stress corrosion crack velocities, namely, $10^{-6}$ to $10^{-9}$ $sec^{-1}$. This strain rate is quite important, as too high a strain rate would result in ductile failure by void coalescense prior to the development of the

necessary corrosion reactions; while too slow a strain rate could again fall out of the range for SCC failures to occur. For these reasons, it is important to realize that the absence of cracking in a given medium does not necessarily preclude the possibility of stress corrosion cracking until additional strain rate tests (both higher and lower values) have been completed.

Twelve CERT tests were performed in different environments, as defined in Table 2. Ten of the specimens were machined in such a manner that the counterbore and weldment were left intact, while two of the specimens were machined flat. The reason for leaving the counterbore and weld root intact was to maintain the inside surface condition of the pipe at the pipe/liquid interface. This method would also give an indication of the effect of any inside surface imperfections on the susceptibility of the material to IGSCC.

Nine of the twelve specimens were tested in a 2000 ppm B (as $H_3BO_3$) solution with additions of $Cl^-$ (varying from 1 to 15 ppm) and MnS additions, and strain rates were in the range of 1.3 to 1.7 x $10^{-6}$ $sec^{-1}$. The solution temperature was maintained at 30°C in an open beaker and the solutions kept stagnant. After each test, a new solution was prepared and the entire apparatus thoroughly cleaned. The tenth and eleventh specimens were tested in air at a strain rate of approximately 8.7 x $10^{-6}$ $sec^{-1}$, while the twelfth specimen was tensile-tested at a strain rate of 1" $min^{-1}$. After the completion of the CERT testing (to fracture) all specimens were cut in order to view the fracture face by SEM, and the opposite side of the specimen mounted in hard epoxy for viewing by optical microscopy. Prior to the optical microscopic examination, all of the specimens were etched by ASTM A262-Practice A (oxalic acid test) for determination of degree of weld sensitization.

Table 2 outlines the results of the CERT testing. From the table it can be seen that five of the twelve failures were identified as either fully or partially intergranular in nature. Four of these occurred in the field weld, while only one intergranular-type failure occurred in the shop weld.

The CERT test, with the MnS addition, resulted in a ductile-type failure with no areas of intergranular fracture. It was noted that during the mixing of the solution with MnS + $H_3BO_3$, $H_2S$ was liberated. The faces of the intergranular-type fractures were characterized by grains which have a dimpled-ruptured appearance on their facets. EDS examination of the dimples showed them to be composed of either MnS or a Ti/Mn (probacarbide) inclusion. These facts suggest that the intergranular-type failure is not a brittle-type failure but more ductile in nature than that observed in the original failed crack.

The microstructures exhibited in the field weld were predominantly of the ditched type (ASTM A262), which is indicative of a highly sensitized material; while the shop weld displayed a predominantly dual type structure, which would indicate a lesser degree of sensitization. This correlates reasonably well to the results of the CERT testing.

It is also interesting to note that of the four shop weld specimens tested, the two that had the weld root and counterbores machined failed in a ductile manner, while only one of the non-machined specimens failed in a similar manner. This suggests that the inside surface condition (after welding) of a stainless steel pipe, or the corrosion films developed during exposure to the fuel pool ccolant, may have an influence on the initiation of IGSCC.

The most significant result obtained during this series of tests is the partially intergranular-type fractures of the air tested field weld specimens (Figure 7). This failure occurred at a strain rate of 8.71 and 8.6 x $10^{-6}$ $sec^{-1}$ and is a definite indication of a highly sensitized structure, which is substantiated by the photos of the microstructures.

ELECTROCHEMICAL POTENTIOKINETIC REACTIVATION ANALYSIS - In an attempt to quantify the degree of sensitization in the area surrounding the repaired portion of the field weld, specimens were cut, mounted and subjected to an Electrochemical Potentiokinetic Reactivation Analysis (EPR Testing). Simply stated, the EPR method is a non-destructive test being developed for determining the degree of sensitization of a stainless steel. It is believed to be correlated to provide useful information for the susceptibility of a material to intergranular stress corrosion cracking.

For ease of calculations, the faces of the samples to be tested were cut to approximately 1 $cm^2$ and all distances were measured from the weld centerline outward to the sample face. All samples were mounted so that the face tested was in a plane parallel to the field weld and contained the cross section area of the pipe. The susceptibility to IGSCC was evaluated electrochemically by performing a controlled potential sweep from the passive to the active region in a 0.5 M $H_2SO_4$ + 0.01 M KSCN solution at 30°C and recording the resultant potentiokinetic curves. The EPR tests were performed using the procedures proposed by G.E. to the ASTM for their "Round Robin" evaluation.

Each of the specimens was polarized to a passivation potential of +200 Mv (SCE) for two minutes and the current recorded during a constant potential sweep at 6 v/h in the

cathodic direction until a potential of -500 mV was reached. Table #3 summarizes the results of the examinations.

The normalized charge per grain boundary area is given by the equation:

$$P_a = Q/GBA \quad (1)$$

where: $P_a$ = Normalized charge per grain boundary area
Q = Integrated current in coulombs
GBA = Grain boundary area, estimated from the ASTM grain size number

As can be seen on the Table, the highest $P_a$ value obtained was approximately 8 mm, (Sample #3) away from the weld centerline (.315 in) which would indicate a significant deree of material sensitization. Sample #6 exhibited a higher $P_a$value than other specimens cut at an equivalent distance from the field weld probably due to its close proximity to the seam weld indicating that, even under controlled shop conditions, this material is somewhat susceptible to sensitization during welding.

Since all of the measurements were done through the cross sectional area of the pipe (through wall) it was necessary to average the grain size for the $P_a$ calculations. The grain size varied from ASTM 1.5 near the pipe's outer surfaces to ASTM 5.5 at its center so a normalized value of 3.5 was used in the calculations. Note - the difference of using ASTM grain size 3.5 in lieu of 5.5 is approximately a multiple of 2.

The values obtained by the EPR tests are well corroborated by the photomicrographs after oxalic acid etching (ASTM A262) and clearly indicated that this particular heat of material #334165 is susceptible to sensitization by welding.

## DISCUSSION

Intergranular corrosion is generally defined as a local attack on the grain boundaries of a metal by a corrosive media.

In stainless steels, susceptibility to intergranular corrosion is greatly enhanced by the sensitization process. Sensitization can be described (in austenitic stainless steels) as the formation of chromium carbide precipitates in the grain boundaries and the resultant depletion of chromium, brought about by heating the steel in the temperature range 500-800°C (1,2).

This temperature range is easily achieved during the welding process where the normal temperature of welding exceeds 1600°C during the fusion welding. Therefore, the welded base material could receive a sensitizing heat treatment in the critical range (500-800°C) at some point outward from the weld fusion time which would be maintained long enough to precipitate chromium carbide at the grain boundaries. This is not to say that the welding process alone will induce a sensitizing effect on the base material, as the degree of material sensitization is a cumulation of the material's prior thermal and mechanical treatments, weld cycle history, (# passes, heat input, etc.) material chemistry, thickness and thermal conductivity, and time at temperatures in the sensitization range.

Residual stresses in a weldment are also an important factor in the stress corrosion cracking phenomenon. An overview paper (3) has cited instances of residual tensile stresses in Type 304 stainless steel heat affected zones of higher than 40 Ksi. The direction and amount of tensile stresses developed in piping seem to be closely related to the pipe's diameter, Chrenko (4) has postulated that the thinner cross sections of smaller diameter pipes provide a less efficient heat sink and a more flexible surface during welding. The heat transferred by welding is then distributed over a larger area with an increased weld shrinkage area resulting in larger axial stresses.

The effect of prior cold working can have a substantial influence on the resistance of a stainless steel to stress corrosion cracking and on its susceptibility to sensitization. Work done by Briant (5) determined that prior cold work increases the material's susceptibility to sensitization, possibly by the formation of a martensitic structure offering a more amenable crystal structure for rapid diffusion of Cr and C and providing a region where chromium depletion takes place. It is also known that cold working produces a stronger layer in the base material which is normally higher in residule stresses than the surrounding metal. It has also been observed (6) that heat treatment conducted at 1050°C for 15 minutes in order to remove the effects of prior cold work has been somewhat effective in reducing the materials susceptibility to stress corrosion cracking.

Thermal cutting of stainless steels can also affect the materials susceptibility to sensitization. Vyas and Isaacs (7) determined that prior plasma arc cutting of 304SS caused a shift in both the location and degree of sensitization after welding. The plasma cutting apparently allowed the material sufficient time at its sensitization temperature to promote chromium carbide nuclei in grain boundaries which grew during the subsequent welding operations.

Since the sensitization process depends upon the depletion of chromium in grain boundaries (1,2) it is a logical conclusion that the reduction of available carbon in the stainless steel (to react with the chromium) would enhance its resistance to sensitization and thus its susceptibility to stress

corrosion cracking. This assumption has been validated by numerous investigations. Kass, Walker, and Giannuizzi (8) observed by varying carbon contents and subjecting 304 and 304L specimens to cyclic loading tests that carbon contents of less than .03% produced no failures after 2000-3000 cycles while carbon contents of .05% or higher produced failures after less than 100 cycles. Failures observed were intergranular in nature.

The effects of various alloying agents (namely S) and subsequently formed inclusions, although investigated, are somewhat less conclusive. Investigations (9,10) do indicate, however, that sulfide inclusions provide possible points for corrosion pit nucleation.

The welding process itself has a most significnt effect on the sensitization process and subsequent susceptibility of type 304 stainless steel to intergranular stress corrosion cracking. Work by Solomon (11) showed that for .05 to .08 w/o C, 304 stainless steel that the critical cooling rate for sensitization is about 5-10°C/S and that for 0.35 in plate thickness and a 30,000 V $in^{-1}$ heat input and cooling rate of 10°C $Sec^{-1}$ can be obtained which would be in the sensitizing range of the material.

The effects of varying chloride concentrations on stainless steel (6,12) below 135°C have produced intergranular cracking in both 304 and 304L stainless steel. Also work by Bednar (13) suggests that alloys of 301 and 305 stainless steel will crack in chloride environments at temperatures between 95 to 154°C, it is, therefore, advisable to reduce or eliminate chloride contamination in contact with stainless steel. Examples of incomplete flushing after hydrochloric acid cleaning have resulted in chloride stress corrosion cracking in 304 and 347 stainless steel (14) in the past. Since there was evidence of grain boundary etching prior cleanup as a possible example of how Cl could have entered the pipe; the results of the CERT tests do indicate, however, that even a concentration of 15 ppm Cl had no adverse affect on the pipe unless it was in an area which was previously highly sensitized; and then, the effects were similar to those found in either pure $H_3O + H_3BO_3$ or air.

High $O_2$ content can also induce stress corrosion cracking in sensitized stainless steels either singly or synergistically with $Cl^-$. van Rooyen and Kendig (15) have proposed that as the electrochemical potential in solution ($O_2$ concentration) is increased; the amount of $Cl^-$ required to cause stress corrosion cracking is decreased. Laboratory cracking of sensitized stainless steel has also been observed (16) in slow strain rate testing; with $O_2$ concentrations of 2 ppm at temperatures as low as 50°C.

In addition to $O_2$ and $Cl^-$, S also seems to play a role in SCC of Type 304 stainless steel. Recent studies by Brookhaven National Laboratory (17) have shown that sensitized Type 304 stainless steel can suffer stress corrosion cracking in low concentrations of thiosulfate solutions at room temperature.

The intergranular-type fracture faces observed in air is quite similar in appearance to those observed by Hippsley, Knott and Edwards (18) on 2 1/4 Cr 1 Mo steel. They attributed the dimpled appearance to the possible decohesion of grain boundary MnS/Matrix interfaces during plastic deformation causing a large amount of cavity nuclei which could induce secondary cracking.

## CONCLUSIONS

1. The primary cause of the cracking appears to be intergranular stress corrosion cracking in the weld sensitized heat affected zone of a weld repair.
2. Although no definite corrosive species were identified as the cause of cracking, the various traces of Cl and S both the pipe inside surface and in the areas of the crack fracture faces detrmined by EDS is evidence of etching and possible contamination of the system by Cl and S ions.
3. The significance of the MnS stringer-like inclusions as pit nucleation sites is inconclusive.
4. The results of Electrochemical Potentiokinetic Reactivation Analysis (EPR) did show at least one area of the pipe's cross section had been sensitized significantly by the welding process.
5. It is evident by the Constant Extension Rate Test (CERT) results (corroborated by the oxalic acid etched microstructures) that the Type 304SS material HT#334165, with its high carbon content and complex thermal history (2 repairs) was severely sensitized at various locations about its girth. This degree of sensitization quantitatively was sufficient to cause intergranular-type fractures during CERT testing in air. This degree of sensitization coupled with the residual stresses from welding and the possible contamination by Cl and S ions were seemingly sufficient to crack the piping by an intergranular stress corrosion cracking mechanism.

## REFERENCES

1. Pande, C.S., Suenage, M., Vyas, B., Isaacs. H.S., and Hailing, D.F., Scripta Metallurgica, 11, 681 (1977)

2. Cowan, R.L. and Tedmon, C.S., Jr., Advances in Corrosion Science and Technology, 3, 293 (1973)
3. Fox, M., Proceedings: Seminar on Countermeasures for Pipe Cracking in BWRs, EPRI, 1 Workshop Report, Paper No. 1. May (1980)
4. Cherenko, M., Proceedings: Seminar on Countermeasures for Pipe Cracking in BWRs, EPRI 2, Workshop Report, Paper No. 21 May (1980)
5. Briant, C.L., Proceedings: Seminar on Countermeasures for Pipe Cracking in BWRs, EPRI, 2, Workshop Report, Paper No. 27 May (1980)
6. Stadder, F., Duquette, D.J., Corrosion, 33, No. 2, 67 February (1977)
7. Vyas, B., Isaacs, H.S., ASTM, Special Technical Publications 656.
8. Kass, J.N., Walker, W.L., Giannuzzi, A.J., Corrosion, 36 No. 6, 299 June (1980)
9. Manning, P.E., Duquette, D.J., Savage, W.F., Corrosion, 36, No. 6, 313 June (1980)
10. Lyle F.F., Jr., Corrosion, 29, No. 3, 86 March (1973)
11. Solomon, H.D., Proceedings: Seminar on Countermeasures for Pipe Cracking in BWRs, EPRI, 2, Workshop Report, Paper No. 24 May (1980)
12. Torchio, S., Corrosion Science, 20, 555 (1980)
13. Bednar, L., Corrosion, 33, No. 9, 321 September (1977)
14. Engle, J.P., Floyd, G.L. Rosene, R.B., NACE Technical Committee Report Publication 59-5, Corrosion, 15, 69t February (1959)
15. van Rooyen, D. Kendig, M.W., BNL-NUREG-28147, Brookhaven National Laboratory, June (1980)
16. Andresen, P., Ford, F.P, Proceedings: Seminar on Countermeasures for Pipe Cracking in BWRs, EPRI, 1, Workshop Report, Paper No. 7 May (1980)
17. Isaacs, H.S., Vyas, B., Kendig, M.W., Unpubslished paper to be presented at NACE, Corrosion (1981)
18. Hippsley, C.A., Knott, J.F., Edwards, B.C., Acta Metallurgica, 28, 869 July (1980)

ACKNOWLEDGEMENTS

The author wishes to thank the USNRC (FIN A3011) for funding this work and R. Sabatini for his SEM/EDAX work, K. Sutter for his aid in the CERT experiments, Dr. B. Vyas for his help in the initial investigations, C. Schnepf and R. Graeser for the metallography and Dr. J.R. Weeks for his helpful discussions and encouragement.

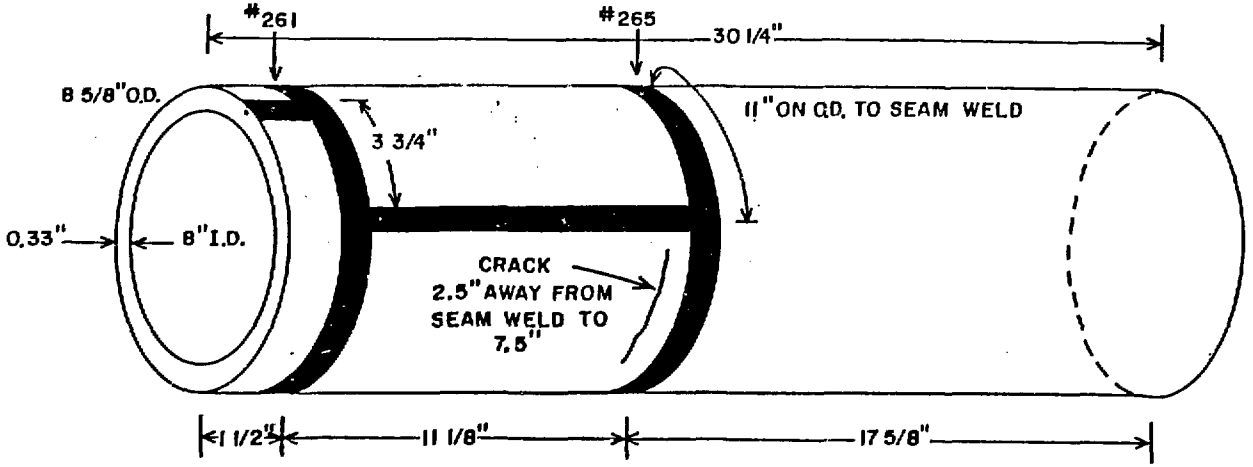


Figure 1. Location of welds and crack on 30¼" piece of 8" stainless steel pipe.

3 MILE ISLAND PIPE
MET. ED.
SCH 40 TY 304
HT 334165
BAL OF 24' 1 3/8"
W 18809

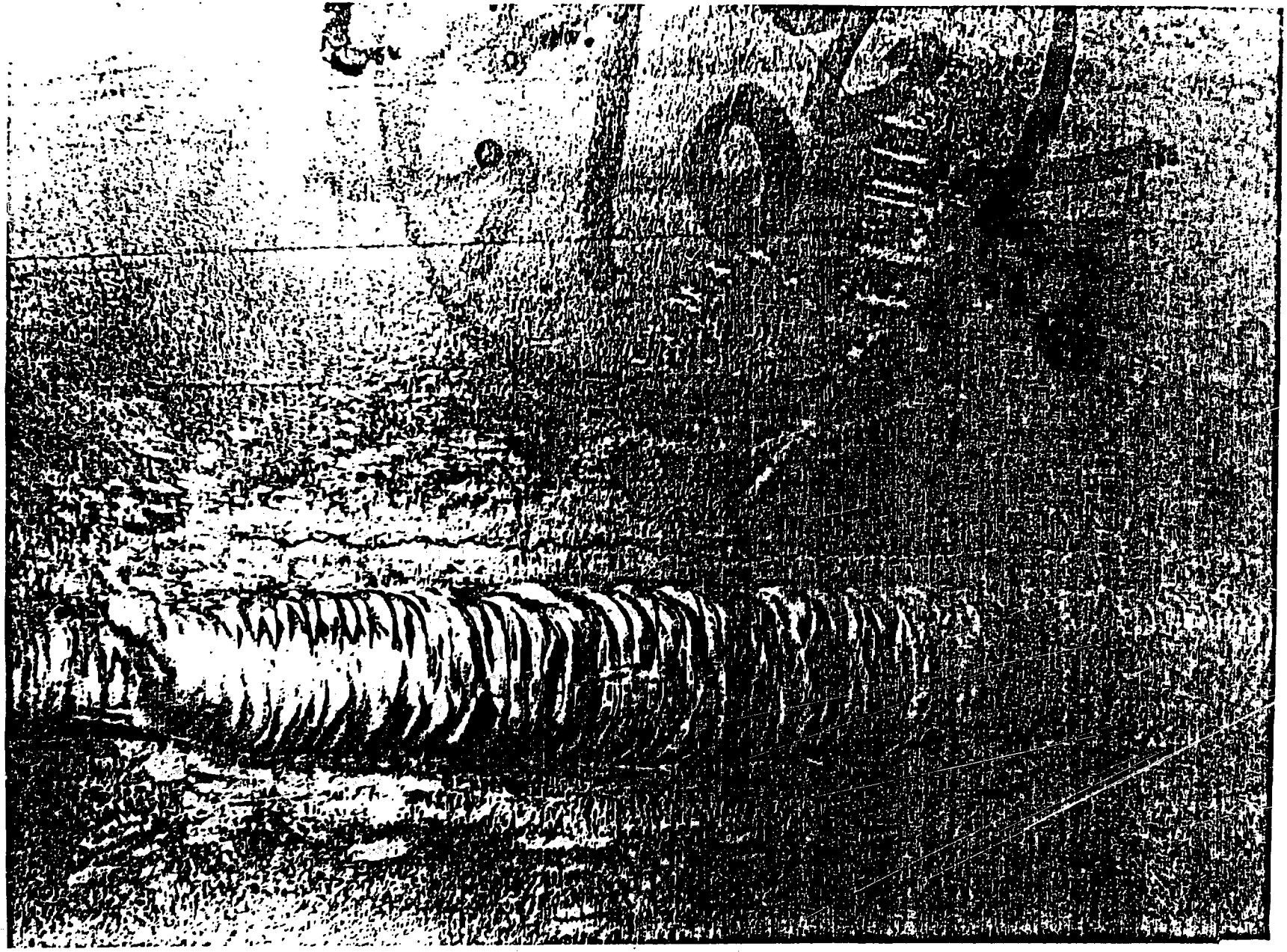

Figure 2. Photograph of crack on 8" diameter pipe outside surface (crack ~5" in length). 1.5X

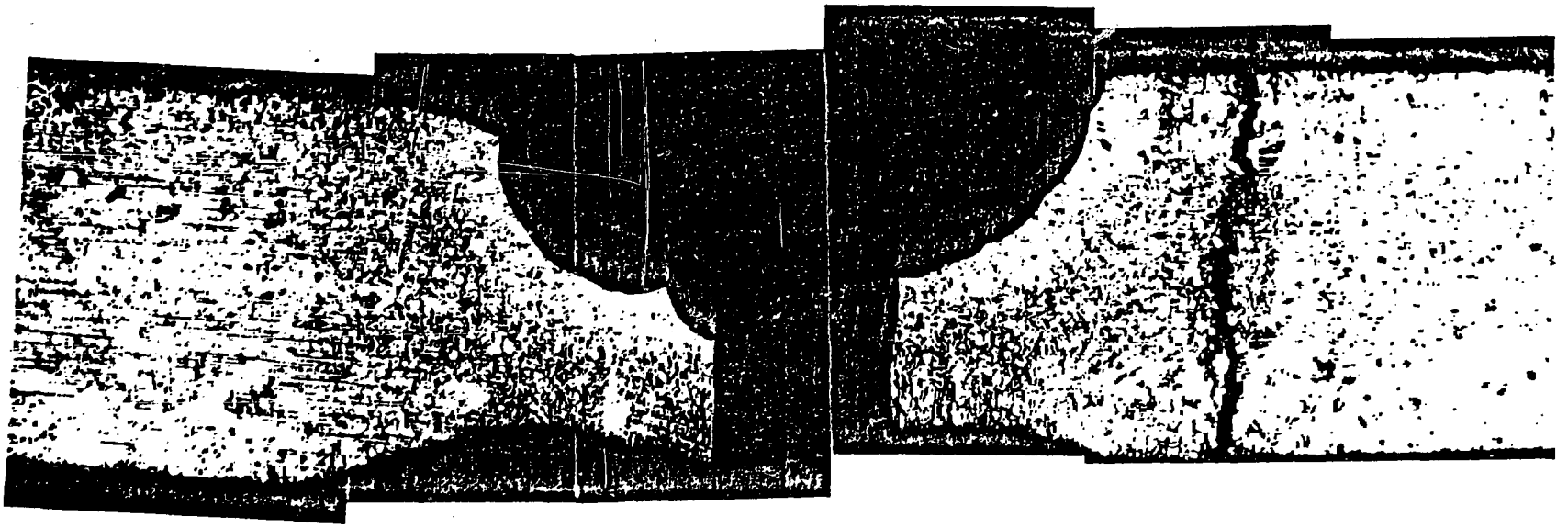

Figure 3 Photomicrograph of specimen showing crack, counterbore and weldment.

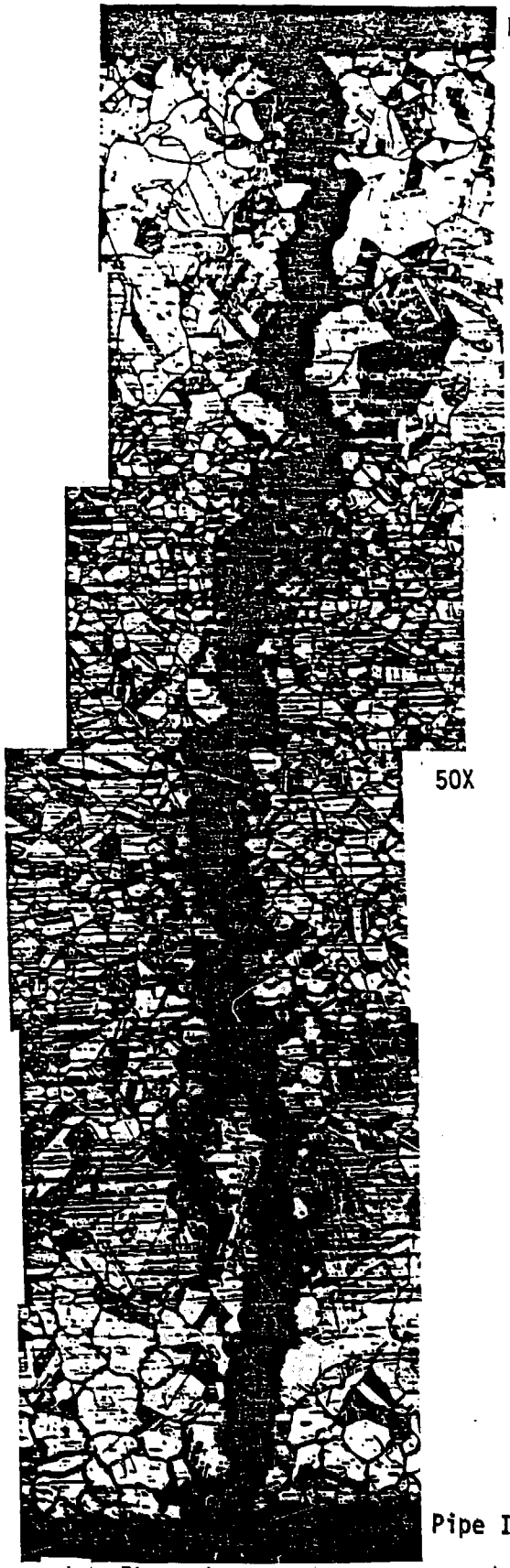


Figure 4 Photomicrograph of crack after ASTM A262 (Practice A) performed.

Fracture surface

100X

Figure 5 SEM photo of "etched" surface on pipe I.D.

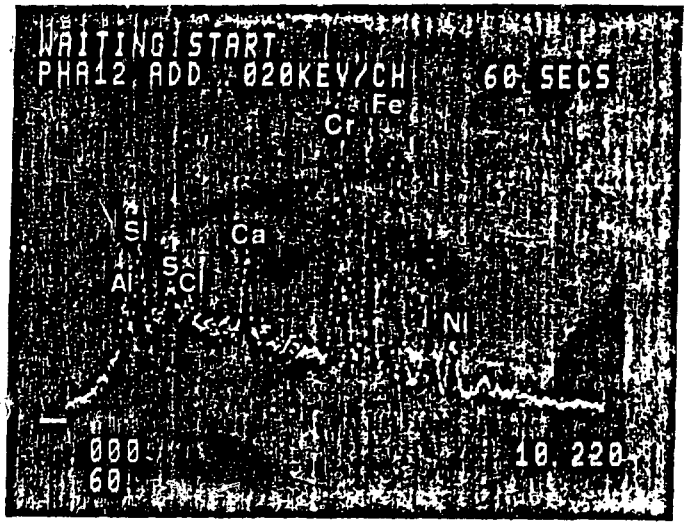


Figure 6 EDS scan of surface near "etched" grain boundaries.

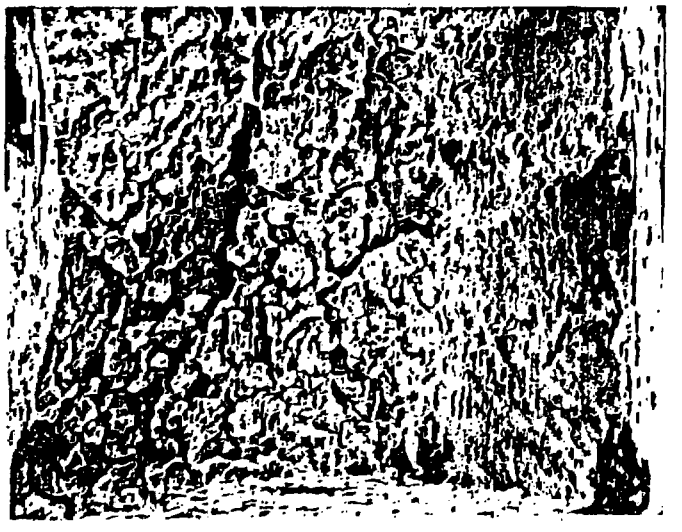

39X

Figure 7 SEM fracture face of CERT #11 tested in air. - Intergranular (~70%) type fracture.